

Structural and optical properties of CdTe/CdSe heterostructure multilayer thin films prepared by physical vapor deposition technique

M. Melvin David Kumar · Suganthi Devadason

Received: 27 May 2012 / Accepted: 20 July 2012 / Published online: 8 August 2012
© The Author(s) 2012. This article is published with open access at Springerlink.com

Abstract CdTe/CdSe heterostructure multilayer thin films and single layers of CdSe and CdTe thin films were prepared. Sequential thermal evaporation technique is made possible to adjust the layer thickness precisely. XRD studies were used to calculate average size of the crystallites and confirmed the (111) and (100) planes of CdTe and CdSe, respectively. Bulk CdTe has band gap energy of 1.54 eV that can be shifted to larger values by reducing the crystallite size to dimensions smaller than the Bohr radius of the exciton. Experimentally measured energy levels show the spin-orbit split of valance band of CdTe. Crystallite sizes (7–12 nm) were calculated with the predictions of effective mass approximation model (i.e., Brus model) which shows that the diameter of crystallites were much smaller than the Bohr exciton diameter (14 nm) of CdTe. It is found that the emission peaks of the prepared CdTe/CdSe ML samples were shifted from the peaks of CdSe and CdTe single layers toward red region as a characteristic of type II band alignment.

Keywords CdSe · CdTe · Multilayer · Heterostructure · Quantum confinement

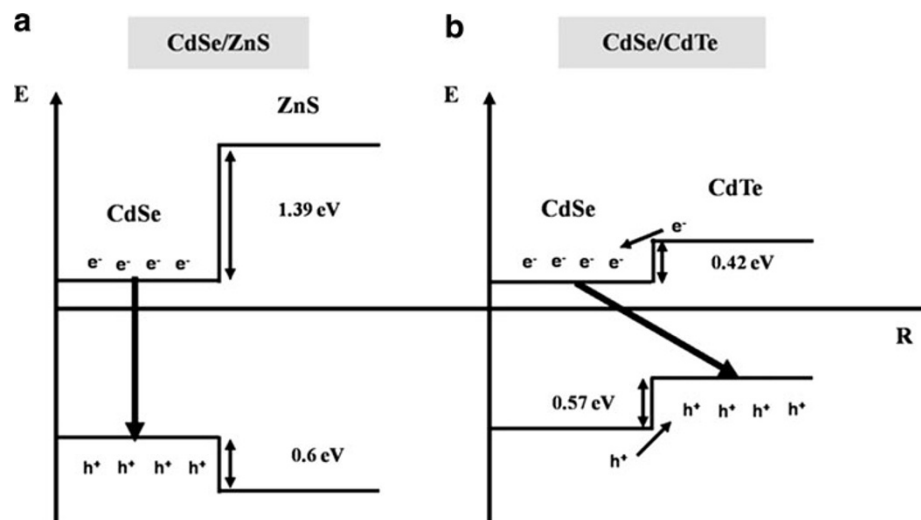
Introduction

Quantum size effects in semiconductors occur when the size of the particle is small in comparison with Bohr excitonic radius which acts as a natural length scale of the electron-hole pair. This effect is a direct consequence of

the confined electron and hole motions in three dimensional spaces. Quantum confinement effect is characterized by discrete energy level structure and electronic transitions which have been shifted to higher energies upon decrease of the size of the particle. Qualitatively this confinement effect is similar to the problem of particle in a box. Size-dependant reactivity (Beck and Siegel 1992), optical non-linearity (Wang and Mahler 1987), efficient photo electron emission (Alfassi et al. 1982) and melting point reduction (Goldstein et al. 1992) are some of the interesting properties exhibited by nano-particles. Size-controlled spectral tunability adds advantage to quantum dots in the fields of optoelectronic devices, bio-labeling and photovoltaic applications (Alivisatos 1998; Gratzel 2000). The nanostructures of II–VI materials such as CdS (Potter and Simmons 1988), CdSe (Nesheva and Levi 1997) and CdTe (Potter and Simmons 1990) have attracted more attention for their great fundamental, experimental and applied interests. Combination of heterostructures form II–VI semiconductors promises the techniques for “band engineering”. Heterostructure multilayer thin films result in the formation of type I and type II band alignments (Lee et al. 2009) as shown in Fig. 1. In Type I heterostructure thin films, the energy levels (valance band and conduction band) of lower band gap semiconductor is placed in between the energy levels of higher band gap semiconductor. Whereas in type II heterostructure thin films, only valance band energy levels of lower band gap semiconductor is kept in between the energy levels of higher band gap semiconductor. The conduction band of lower band gap material is seen above the conduction band of higher band gap semiconductor. Type II heterostructure nanocrystals spatially separates photo-generated carriers within the nanostructure such that the electron wave function mainly resides in one semiconductor and hole wave function in the other (Milliron

M. M. David Kumar (✉) · S. Devadason
Thin Film Laboratory, Department of Physics, Karunya
University, Coimbatore 641 114, India
e-mail: melvin@karunya.edu

Fig. 1 Schematic diagrams of **a** type I and **b** type II heterojunction band alignment



et al. 2004). Recent investigations of type II CdTe/CdSe heterostructure nanocrystallites are ideal materials for their long range photo-induced charge separation and could be applied in photovoltaic devices (Lee et al. 2009; Kumar et al. 2007; Peng et al. 2005). CdSe, CdTe and CdTe/CdSe tetrapod nanocrystals perform well in nanocrystal–polymer hybrid solar cells (Huynh et al. 2002; Sun et al. 2003; Gur et al. 2007). Few researchers have prepared type II CdTe/CdSe tetrapod nanocrystals in chemical synthesis route (Wang and Han 2010; Saad et al. 2011; Kim et al. 2003). In the present work, we report the formation of type II nanocrystals in CdTe/CdSe multilayer thin films prepared by physical vapor deposition method where thickness of each layer can be controlled accurately up to few nanometers. Alternating coating of CdTe and CdSe heterostructure semiconductors under high vacuum condition provides an uniform sequential arrangement of layers in the order of few nanometers so that trapping of electron–hole pair is made possible in simple steps. Crystallite sizes calculated by both Debye–Scherrer formula and effective mass approximation of Brus model were smaller than the Bohr excitonic radius. It has been generally proved that the quantum confinement effect should be observable if the radius of nano crystallites becomes less than the Bohr excitonic radius for corresponding material.

Experimental details

CdTe/CdSe nanocrystalline multilayer thin films were prepared by consecutive thermal evaporation of CdSe and CdTe (99.99 % Aldrich Chem. Co.) from two independent molybdenum crucibles in vacuum condition at a pressure of 5×10^{-5} mbar. Glass substrates were used for coating thin film samples and were not intentionally heated. The nominal film thickness and deposition rate of each sublayer were controlled by calibrated digital thickness monitor (DTM). The

Table 1 Details of the CdSe/CdTe multilayer thin film samples preparation

S. no	Name of the sample	Total number of layers in the sample	Order of sublayers		Thickness of sublayers (Å)		Total thickness of the film (Å)
			Bottom layer	Top layer	CdTe	CdSe	
1	CdSe	1	CdSe	–	–	–	500
2	CdTe	1	CdTe	–	–	–	500
3	S1	10	CdTe	CdSe	100	100	1,000
4	S2	7	CdTe	CdTe	1,000	100	4,300
5	S3	10	CdTe	CdSe	500	200	3,500

substrates were fixed at the greatest possible distance for which the tooling factor was calculated. Step-by-step procedure was applied in the deposition of each sublayer in the multilayer structures. We prepared CdSe and CdTe single layer thin films with 50 nm thickness as reference films and three CdTe/CdSe multilayer thin film samples namely S1, S2, and S3 with different sublayer thicknesses as given in Table 1, to find out the changes taking place in the structural and optical properties. The structural properties of the samples were analyzed by X-ray diffractometer (JEOL 60 PA XRD) and scanning electron microscope (Hitachi S3200). The absorption and emission properties of the samples were studied using UV–VIS spectrophotometer (Hitachi 3010) and photo luminescence spectrometer (Hitachi F-2500), respectively.

Results and discussion

Structural analysis using XRD and SEM

Structural properties of CdTe/CdSe multilayer thin films coated under specific conditions were analyzed using X-ray

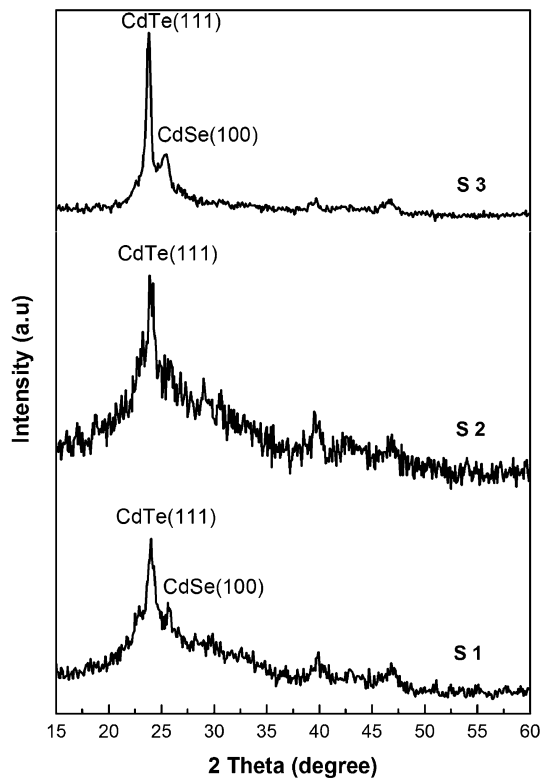


Fig. 2 X-Ray diffraction pattern of CdTe/CdSe heterostructure multilayer thin film samples S1, S2 and S3

diffraction spectra. XRD measurements allowed the identification of the nanocrystalline phases and the determination of the average crystallite sizes. The XRD profiles for the samples S1, S2 and S3 are shown in Fig. 2. Broadness of the XRD peak indicates that the size of the crystallites is very small (Arizpe-Chavez 2000). Since the thickness of each sublayer and the size of the crystallites are in the order of few nanometers, the XRD spectra have small spike-like structures throughout the range. A prominent peak approximately at 24.5° appears in all the spectra referring [JCPDS-89-3011] to (111) plane of the CdTe with cubic structure. An additional peak approximately at 25° referring [JCPDS-88-2346] to (100) plane of CdSe with wurtzite structure is observed in the samples S1 and S3 since CdSe was coated as top layer in few nanometer thickness intentionally in those samples. In the samples S2, the peak corresponding to CdSe was concealed, as X-rays get diffracted mainly from top surface. This confirms the presence of CdTe and CdSe with zinc blende and wurtzite structures, respectively, in all CdTe/CdSe heterostructure multilayer thin films. The average sizes of nanocrystallites were determined using Scherer's expression (Klug and Alexander 1954).

$$D = \frac{0.94\lambda}{\beta \cos \theta}, \quad (1)$$

Table 2 Size of the crystallites calculated from XRD data

S. no	Sample	2θ ($^\circ$)	d (\AA)	FWHM ($^\circ$)	D (nm)
1	S1	24.45	3.63776	1.59935	5
2	S2	24.4750	3.63410	1.31315	6
3	S3	23.7682	3.74054	0.5705	14

where D is the crystallite size, λ is the wavelength of X-ray, β is the full width at half maximum (FWHM) after correcting the instrument peak broadening (β expressed in radians), and θ is the Bragg's angle. This method provides an estimation of the CdSe crystallite size with a maximum error of about 20 % (Arizpe-Chavez 2000). Calculated size of the nanocrystallites was in between 5 and 14 nm and is tabulated in Table 2. Usually one can expect quantum size effect in this range. Surface images of CdTe/CdSe heterostructure multilayer thin film were recorded using scanning electron microscope (SEM) shown in Fig. 3. The particles are smoothly and uniformly distributed on the surface. It is seen that the cluster of particles have formed batches on the surface of the samples.

Optical properties of CdTe/CdSe heterostructure multilayer thin films

Absorption spectra of CdSe, CdTe single-layer thin films and CdTe/CdSe ML samples S1, S2 and S3 were shown in Fig. 4a and b, respectively. The absorption edges of the CdTe/CdSe ML samples gradually shifted from 697 to 766 nm when the thicknesses of sublayers are changed. Since the CdTe/CdSe ML system exhibits type II band alignment, the possible electronic transitions may take place between valance bands of CdTe to conduction band of CdSe (Milliron et al. 2004). The energy corresponding to the possible electronic transition in non-quantized type II CdTe/CdSe system will be lesser than the band gaps of both the mentioned semiconductors. But these electronic transitions can be shifted to higher energies upon decrease of particle size (Pejova 2008). Substructures are seen in the absorption spectra of CdTe/CdSe ML samples (Fig. 4b) but not in the spectra of CdTe and CdSe single-layer thin films (Fig. 4a), which may be related to electronic transitions between discrete hole and electron energy levels in the valance and conduction bands due to spin-orbit coupling (Nesheva et al. 2002). As a result of spin-orbit interaction, valance band of CdTe semiconductor splits into an energetically higher and lower components which were usually labeled as Γ_7^v and Γ_8^v . Transition energies between valance bands and conduction band of CdTe/CdSe ML samples S1, S2 and S3 were calculated by plotting a typical graph between energy ($h\nu$) and $(\alpha h\nu)^2$ as shown in Fig. 5 using the following relation (Tauc 1979),

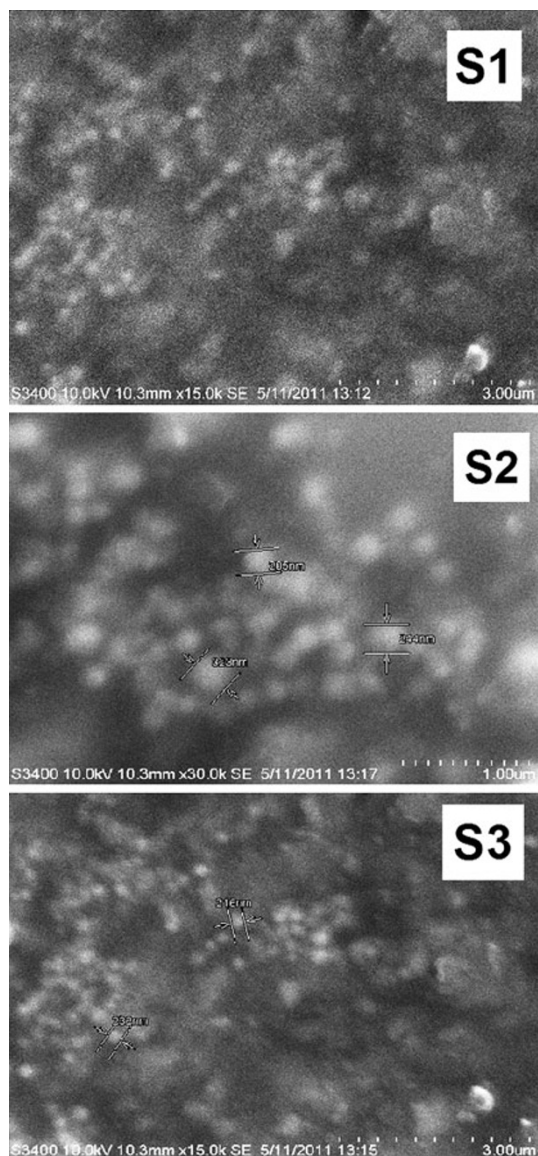


Fig. 3 Scanning electron microscope images of CdTe/CdSe ML samples showing distribution of the particles on the surface

$$(\alpha hv)^2 = A(hv - E_g)^n. \quad (2)$$

In Eq. (2), A is a constant which arises from Fermi's golden rule for fundamental band-to-band electronic transitions and exponent $n = 1/2$ (for the electronic transitions with the energy values quiet straightforward. According to the direct allowed transition). Two electronic transitions were observed in Fig. 5a, b and c rather than obtaining a single transition as in bulk CdSe and CdTe material. The transitions close to the fundamental band gap (E_g) of II–VI semiconductors arise due to the spin–orbit split of valance band energy levels (Baldereschi and Lipari 1971). Based on the model proposed by Chestnoy et al. (1986), the

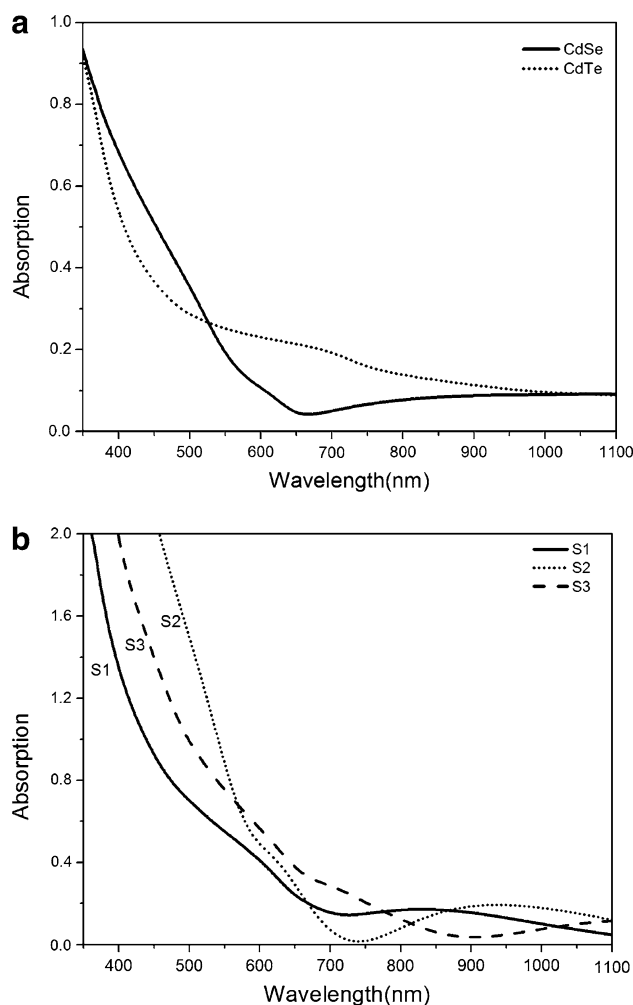


Fig. 4 **a** Absorption spectra of CdSe and CdTe single layer thin films. **b** Absorption spectra of CdTe/CdSe ML samples indicating the shift of absorption edges

valance band components Γ_7^v and Γ_8^v are expected to give rise to one set of discrete hole states separately as depicted in Fig. 6. This proposed model has made the task of assigning energy order, the obtained energy values in sample S1 (1.78 and 1.98 eV), S2 (1.7 and 1.88 eV) and in S3 (1.62 and 1.8 eV) given in Fig. 5a, b and c may be attributed to the transitions take place between $1S-1S$ and $1S\Delta-1S$ energy states, respectively (Pejova and Grozdanov 2005; Woggon et al. 1996). The calculated band gap energies (E_g) as given in Table 3 are higher than the band gap of bulk CdTe ($E_{g(\text{bulk})}$) i.e., 1.54 eV at room temperature (Sharmaa 2005). As it can be seen from Table 3, the confinement energies ($E - E_{g(\text{bulk})}$) for the samples S1, S2 and S3 are large which states that the prepared ML samples are strongly quantized (Pejova and Grozdanov 2005). Size of the particles can be calculated from the band gap shift ($E_g - E_{g(\text{bulk})}$) with respect to bulk band gap value of CdTe using Brus effective mass approximation equation as given,

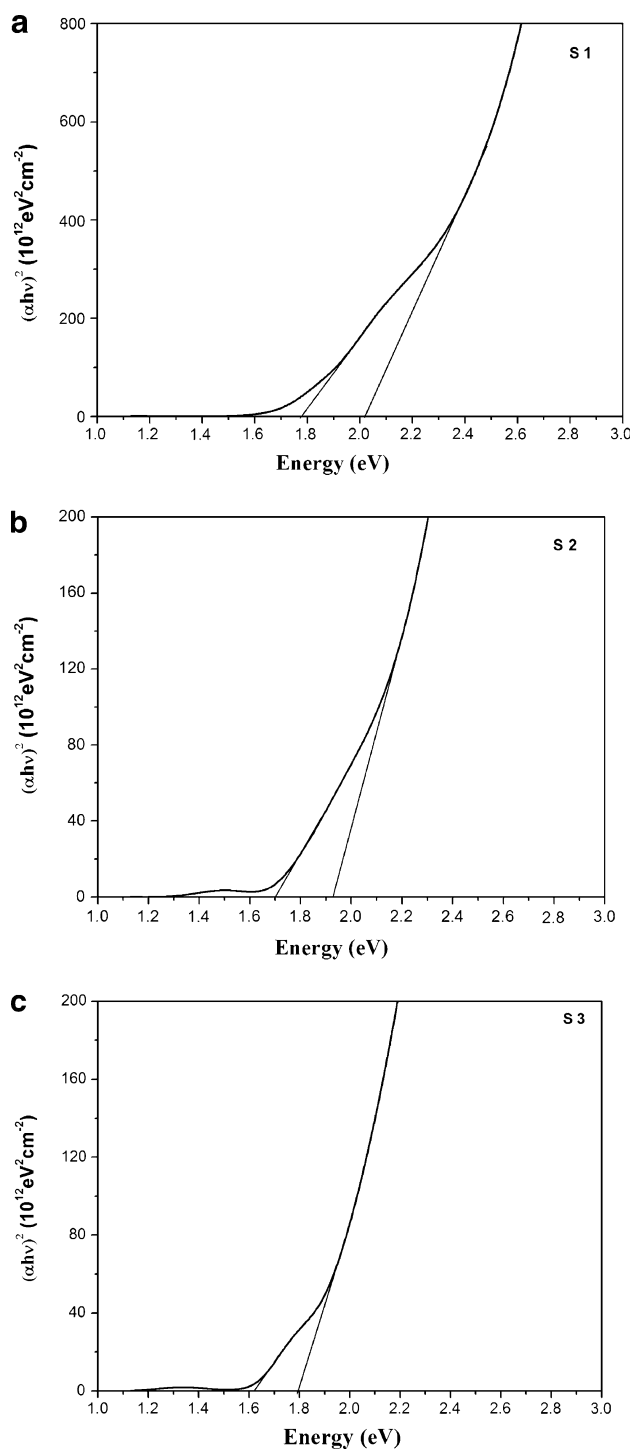


Fig. 5 The plots of (αhv) versus $(\alpha hv)^2$ graph for the samples S1 (a), S2 (b) and S3 (c) with $\Gamma_7^v-\Gamma_6^v$ and $\Gamma_8^v-\Gamma_6^v$ transitions

$$E_g = E_{g(\text{bulk})} + \frac{2\hbar^2 \pi^2}{\mu d^2}, \tag{3}$$

where E_g is the band gap values obtained from experiment, $E_{g(\text{bulk})}$ is the band gap of bulk CdTe (=1.54 eV), d is the

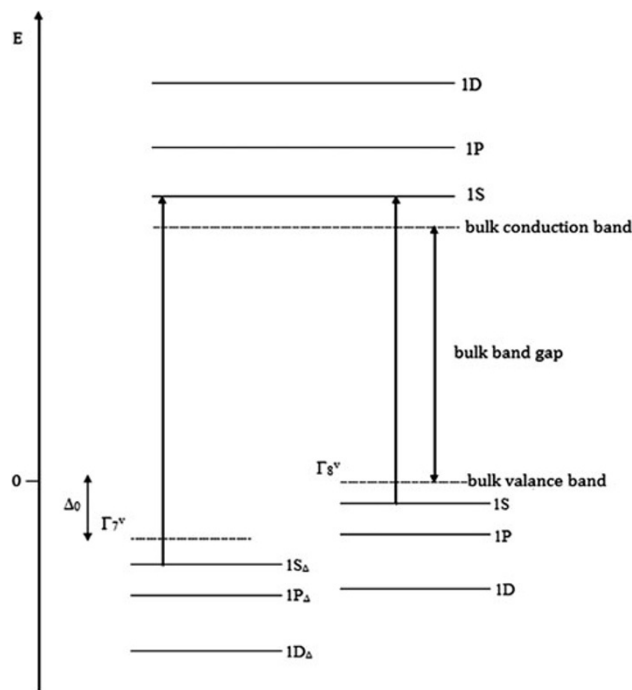


Fig. 6 The discrete hole and electron states arising from valence and conduction bands in the case of CdTe semiconductor (Chestnoy et al. 1986)

diameter of the crystallites and μ is the effective mass of electron–hole pair given by,

$$\frac{1}{\mu} = \frac{1}{m_e^*} + \frac{1}{m_h^*}, \tag{4}$$

where m_e^* and m_h^* are effective mass of electron and hole, respectively. It has been generally proven that the quantum confinement effect should be observable if the radius of nanocrystallites becomes less than the Bohr excitonic radius of the corresponding material. The bulk Bohr diameter of the Wannier exciton in CdTe is 14 nm (Sharma 2005). The average size of the nanocrystallites calculated using Eq. (3) varies between 7 to 12 nm and tabulated in Table 3. It is evident that the nanocrystallite sizes (D_o) of the CdTe/CdSe heterostructure multilayer thin film samples are much smaller than the Bohr exciton diameter (D_B). If $D_o/D_B \ll 2$, the crystal exhibits a single particle confinement behavior in which electrons and holes are independently confined. Hence, the prepared CdTe/CdSe heterostructure multilayer thin films confirm the quantum confinement effect. Size of the crystallites calculated from effective mass approximation is not precisely matched with the size of the crystallites calculated from X-ray diffraction spectra. In order to explain the observed discrepancy one should take into account that the full width at half maximum of X-ray diffraction peaks depends not only on the nanocrystal size but also on existing

Table 3 Size of the crystallites from UV–Vis data by Brus model

S. no	Sample	$E (\Gamma_7^v-\Gamma_6^c)$ (eV)	$E_g (\Gamma_8^v-\Gamma_6^c)$ (eV)	$(E-E_g)$ eV	$(E-E_{g(\text{bulk})})$ eV	Shift in band Gap $(E_g-E_{g(\text{bulk})})$ eV	D (nm)
1	S1	1.98	1.78	0.20	0.44	0.24	7
2	S2	1.88	1.7	0.18	0.34	0.16	9
3	S3	1.8	1.62	0.18	0.26	0.08	12

microstrains and deformations in the nanocrystal arrangement (Sen et al. 1975).

Luminescent property

The emission spectra were recorded for CdTe/CdSe heterostructure multilayer thin film samples S1, S2 and S3 shown in Fig. 7. The emission peaks of CdTe/CdSe samples are observed at longer wavelengths than that of the individual layers as it is the characteristic feature of type II quantum dots. It is found that the intensity of emission peak and smoothness increase when the particle size increases. Moreover, the emissions of the CdTe/CdSe heterostructure samples are more structured than the individual CdSe and CdTe bands. There is a splitting of the emission maximum observed with the bands centered on

410 and 435 nm in ML samples. This might be the presence of CdSe and CdTe individual peaks appear together with shifting in longer wavelength side. In this type of heterostructure multilayer thin films, the energy of the emission thus depends on the band offsets of the two materials (lesser band gap and higher band gap) and can emit at energies smaller than the band gap of either material. The FWHM of the ML samples is another noteworthy entity. FWHM of CdTe/CdSe ML samples are larger than 40 nm, which is far larger than that of ordinary bulk semiconductor sample. The main reason of this phenomenon is the size fluctuation of the quantum dots (Mao et al. 2005). The FWHM of the CdTe/CdSe ML sample S1 is the largest one, because the size of the particle in this sample is smallest and the quantum confinement effect is most notable. The large Stokes shift between the absorption maximum and the PL band may be due to the presence of at least one deep trapping site and electron–hole recombination via trap state (Chaurea and Chaurea 2005).

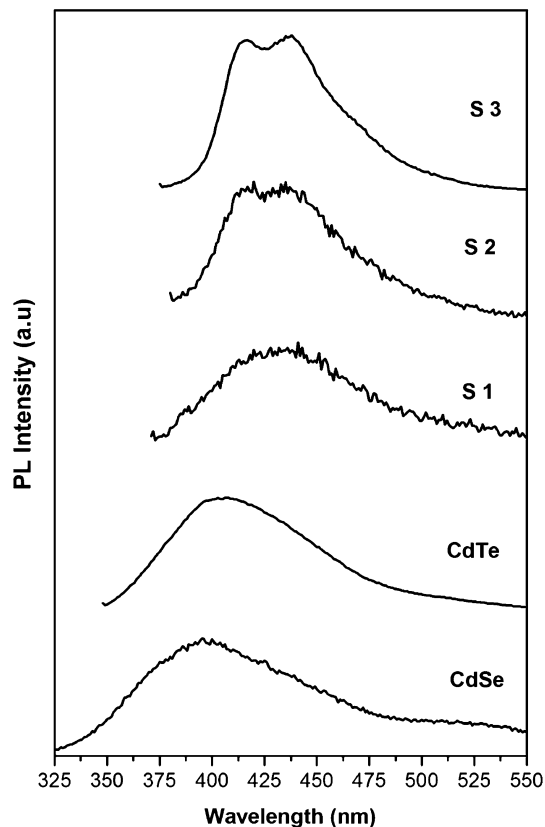


Fig. 7 Photoluminescence Spectra of CdTe/CdSe ML samples S1, S2 and S3 along with CdSe and CdTe single layers

Conclusion

CdTe/CdSe multilayer thin films with various sublayer thicknesses were prepared using physical vapor deposition technique. This method gives the possibility of preparing nanocrystals of various semiconductors with a relatively smaller size distribution in relatively shorter times than the conventional method. Quantum confinement effect was explained in connection with structural and optical properties of CdTe/CdSe ML systems. Spin–orbit split of valance band of CdTe was discussed from absorption spectra and $(h\nu)$ versus $(\alpha h\nu)^2$ graph. We conclude that the sublayer thickness in ML systems is one of the factors which plays a role in quantum confinement effect and FWHM is a size-dependent quantity which changes with change of the particle size. Further studies will be carried out with type I band structure multilayer systems in order to explain the interdot coupling between the quantum dots through tunneling effect.

Acknowledgments The authors are thankful to the Management and the Central Research Facility of Karunya University for their support for this research.

Open Access This article is distributed under the terms of the Creative Commons Attribution License which permits any use, distribution, and reproduction in any medium, provided the original author(s) and the source are credited.

References

- Alfassi Z, Bahnemann D, Henglein A (1982) Photoelectron emission from cadmium sulfide and cadmium sulfide–zinc sulfide colloids. *J Phys Chem* 86:4656
- Alivisatos AP (1998) Electrical studies of semiconductor-nanocrystal colloids. *MRS Bull* 23:18
- Arizpe-Chavez H (2000) Quantum confinement effects in CdTe nanostructured films prepared by the RF sputtering technique. *J Phys Chem Solids* 61:511–518
- Baldereschi A, Lipari NG (1971) Energy levels of direct excitons in semiconductors with degenerate bands. *Phys Rev B* 3:439
- Beck DD, Siegel RW (1992) The dissociative adsorption of hydrogen sulfide over nanophase titanium dioxide. *J Mater Res* 7:2840
- Chaurea S, Chaurea NB, Pandey RK (2005) Self-assembled nanocrystalline CdSe thin films. *Physica E* 28:439–446
- Chestnoy N, Hull R, Brus LE (1986) Higher excited electronic states in clusters of ZnSe, CdSe, and ZnS: Spin-orbit, vibronic, and relaxation phenomena. *J Chem Phys* 85:2237
- Goldstein AN, Echer CM, Alivisatos AP (1992) Melting in semiconductor nanocrystals. *Science* 256:1425
- Gratzel M (2000) In: Nalwa HS (ed) *Handbook of Nanostructured Materials and Nanotechnology*, vol 3. Academic Press, San Diego, p 527
- Gur I, Fromer NA, Chen C-P, Kanaras AG, Alivisatos AP (2007) Hybrid solar cells with prescribed nanoscale morphologies based on hyperbranched semiconductor nanocrystals. *Nano Lett* 7:409–414
- Huynh WU, Dittmer JJ, Alivisatos AP (2002) Hybrid nanorod-polymer solar cells. *Science* 295:2425–2427
- Kim S, Fisher B, Eisler H-J, Bawendi M (2003) Type-II quantum dots: CdTe/CdSe(core/shell) and CdSe/ZnTe(core/shell) heterostructures. *J Am Chem Soc Commun* 125:11466–11467
- Klug HP, Alexander LE (1954) *X-ray diffraction procedures*. Wiley, New York
- Kumar S, Jones M, Lo SS, Scholes GD (2007) Nanorod heterostructures showing photoinduced charge separation. *Small* 3: 1633–1639
- Lee H, Yoon SW, Ahn JP, Suh YD, Lee JS, Lim H, Kim D (2009) Synthesis of type II CdTe/CdSe heterostructure tetrapod nanocrystals for PV applications. *Sol Energy Mater Sol Cells* 93:779–782
- Mao H, Chen J, Wang J, Li Z, Dai N, Zhu Z (2005) Photoluminescence investigation of CdSe quantum dots and the surface state effect. *Physica E* 27:124–128
- Milliron DJ, Hughes SM, Cui Y, Manna L, Li JB, Wang LW, Alivisatos AP (2004) Colloidal nanocrystal heterostructures with linear and branched topology. *Nature* 430:190–195
- Nesheva D, Levi Z (1997) Nanocrystals of CdSe in thin film SiO_x matrix. *Semicond Sci Technol* 12:1319
- Nesheva D, Hofmeister H, Levi Z, Aneva Z (2002) Nanoparticle layers of CdSe buried in oxide and chalcogenide thin film matrices. *Vacuum* 65:109–113
- Pejova B (2008) The higher excited electronic states and spin-orbit splitting of the valence band in three-dimensional assemblies of close-packed ZnSe and CdSe quantum dots in thin film form. *J Solid State Chem* 181:1961–1969
- Pejova B, Grozdanov I (2005) Three-dimensional confinement effects in semiconducting zinc selenide quantum dots deposited in thin-film form. *Mater Chem Phys* 90:35–46
- Peng P, Milliron DJ, Hughes SM, Johnson JC, Alivisatos AP, Saykally RJ (2005) Femtosecond spectroscopy of carrier relaxation dynamics in type IICdSe/CdTe tetrapod heteronanostructures. *Nano Lett* 5:1809–1813
- Potter BG Jr, Simmons JH (1988) Quantum size effects in optical properties of CdS-glass composites. *Phys Rev B* 37:10838
- Potter BG Jr, Simmons JH (1990) Quantum-confinement effects in CdTe-glass composite thin films produced using rf magnetron sputtering. *J Appl Phys* 68:1218
- Saad AM, Bakr MM, Azzouz IM, Abou Kana MTH (2011) Effect of temperature and pumping power on the photoluminescence properties of type-II CdTe/CdSe core-shell QDs. *App Surf Sci* 257:8634–8639
- Sen S, Halder SK, Gupta SPS (1975) An X-ray line broadening analysis in the vacuum-evaporated silver films. *J Phys Soc Jpn* 38:1641
- Sharma SN, Kohlib S, Rastogia AC (2005) Quantum confinement effects of CdTe nanocrystals sequestered in TiO₂ matrix: effect of oxygen incorporation. *Physica E* 25:554–561
- Sun B, Marx E, Greenham NC (2003) Photovoltaic devices using blends of branched CdSe nanoparticles and conjugated polymers. *Nano Lett* 3:961–963
- Tauc J (1979) *Amorphous and liquid semiconductors*. Plenum press, New York
- Wang J, Han H (2010) Hydrothermal synthesis of high-quality type-II CdTe/CdSe quantum dots with near-infrared fluorescence. *J Colloid Interface Sci* 351:83–87
- Wang Y, Mahler W (1987) Degenerate four-wave mixing of CdS/polymer composite. *Opt Commun* 61:233
- Woggon U, Wind O, Gindele F, Tsitsishvili E, Muller M (1996) Optical transitions in CdSe quantum dots: From discrete levels to broad gain spectra. *J Lumin* 70:269